Biomaterials 33 (2012) 1180–1189

Contents lists available at SciVerse ScienceDirect

Biomaterials

journal homepage: www.elsevier.com/locate/biomaterials

Gold nanoparticles functionalized with therapeutic and targeted peptides for cancer treatment

Anil Kumar [1], Huili Ma [1], Xu Zhang, Keyang Huang, Shubin Jin, Juan Liu, Tuo Wei, Weipeng Cao, Guozhang Zou, Xing-Jie Liang*

CAS Key Laboratory for Biomedical Effects of Nanomaterials and Nanosafety, National Center for Nanoscience and Technology, Chinese Academy of Sciences, Beijing 100190, PR China

ARTICLE INFO

Article history:
Received 30 September 2011
Accepted 20 October 2011
Available online 5 November 2011

Keywords:
Gold nanoparticles (*Au*NPs)
Therapeutic peptide PMI (p12)
Targeted peptide (CRGDK)
Neuropilin-1 (Nrp-1) receptor
p53 mechanism
Cancer treatment

ABSTRACT

Functionalization of nanostructures such as gold nanoparticles (*Au*NPs) with different biological molecules has many applications in biomedical imaging, clinical diagnosis and therapy. Researchers mostly employed *Au*NPs larger than 10 nm for different biological and medicinal applications in previous studies. Herein, we synthesized a novel small (2 nm) *Au*NPs, which were functionalized with the therapeutic peptide, PMI (p12), and a targeted peptide, CRGDK for selective binding to neuropilin-1(Nrp-1) receptors which overexpressed on the cancer cells and regulated the process of membrane receptor-mediated internalization. It was found that CRGDK peptides increased intracellular uptake of *Au*NPs compared to other surface conjugations quantified by ICP-MS. Interestingly, CRGDK functionalized *Au*NPs resulted in maximal binding interaction between the CRGDK peptide and targeted Nrp-1 receptor overexpressed on MDA-MB-321 cell surface, which improved the delivery of therapeutic P12 peptide inside targeted cells. *Au*@p12 + CRGDK nanoparticles indicated with highly effective cancer treatment by increasing p53 expression upregulated with intracellular enhanced p12 therapeutic peptide. These results have implications to design and functionalize different molecules onto *Au*NPs surfaces to make hybrid model system for selective target binding as well as therapeutic effects for cancer treatment.

1. Introduction

In the recent years, gold nanoparticle (*Au*NPs) based nanocarriers have emerged as attractive candidates for delivery of various payloads into their targets [1,2]. The payloads could be small drug molecules or large biomolecules like proteins, DNA or RNA [3]. *Au*NPs with different shapes and sizes (usually over 10 nm diameter) exhibit their unique physical and chemical properties for transporting and unloading the pharmaceuticals. Firstly, the gold core is essentially inert and non-toxic [4]. Secondly, their ease of synthesis is relatively advantageous provided that mono-disperse nanoparticles (NPs) can be formed with core sizes ranging from 1 to 150 nm. Thirdly, their physicochemical properties could trigger drug release at remote places [5]. Cells themselves have very unique properties to control their function through numerous processes such as intracellular signaling which is triggered by the binding of ligand molecules with cell surface receptors. The level of receptor–ligand binding and receptor cross-linking response activates the various signaling processes and thereby aides the transportation of drugs and other therapeutic molecules into the cells by receptor-mediated endocytosis [6,7]. Recent works reported in various literatures suggest that physical parameters of *Au*NPs can significantly induce cellular responses even with nonspecific binding or uptake inside the cells [8,9].

The *Au*NP-coated TNFα, termed as CYT-6091, have added clinical significance, because it is the first *Au*NPs-based novel nanomedicine that underwent *Phase I* dose escalation clinical trials in advanced stage cancer patients [10]. The biodistribution and pharmacokinetic studies suggest that CYT-6091 delivers TNFα preferentially at the tumor site, while the *Au*NPs are cleared by the liver in a slow phase after TNFα degradation [11]. Biological molecules through recognition of certain peptides, e.g., nuclear localization signaling peptide (NLSs), cell penetrating peptide (CPPs), and receptor-targeted peptides could help in the translocation of *Au*NPs and therapeutic molecules into the cell or nucleus [12]. Currently, ultra-small *Au*NPs conjugated with various payloads have been attracting scientific communities for delivery purpose

* Corresponding author. Chinese Academy of Sciences, Key Laboratory for Biomedical Effects of Nanomaterials and Nanosafety, National Center for Nanoscience and Technology, No. 11, First North Road, Zhongguancun, Beijing 100190, PR China. Tel.: +86 1082545569; fax: +86 10 62656765.
E-mail address: liangxj@nanoctr.cn (X.-J. Liang).
[1] These authors contributed equally to this work.

0142-9612/$ – see front matter © 2011 Elsevier Ltd. All rights reserved.
doi:10.1016/j.biomaterials.2011.10.058

Table 1
Peptide sequences used for conjugation with *Au*@tiopronin.

Peptide	Target	Sequence
Therapeutic (p12)	MDM2	TSFAEYWNLLSP
Target (CRGDK)	Neuropilin-1 (Nrp-1)	CRGDK

especially in cancer cells due to their small size, simple and straight forward process of synthesis as well as high water solubility and stability in physiological conditions.

Peptide functionalized *Au*NPs as nanocarriers have tremendous growth in the pharmaceutical field for intracellular drug and gene delivery, mainly due to their large interacting surface, offering indispensible advantages to enhance potency, high specificity and low toxicity [13,14]. Herein, we have made the first approach with ultra-small *Au*NPs (2 nm) conjugated with therapeutic peptide, PMI and neuropilin-1(Nrp-1) receptor-targeted peptide (Table 1) for cancer treatment. PMI also widely known as p12, is the most known potent inhibitor binding to MDM2 and MDMX complexes resulting in regulated activity and stability of tumor suppressive protein, p53 [15]. p53 is the known protein that transcriptionally regulates the expression of various target gene in response to cellular stress, which indirectly results in the cell cycle arrest, DNA damage or apoptosis [16]. MDM2 (a master regulator) and its homolog MDMX play an important role in regulating and maintaining the stability or integrity of the p53 pathway [17].

Targeted peptide (CRGDK) binding to the Nrp-1 is thought to act as a co-receptor for VEGF by forming complexes with the VEGF protein tyrosine kinase receptor, VEGFR2 (VEGF receptor2)/KDR (kinase insert domain-containing receptor), resulting in enhanced VEGFR2 activation, intracellular signaling, cell migration and angiogenesis in breast cancer [18]. The neuropilin, Nrp-1, is a focus of tumor biological studies because of its involvement in vascular and lymphatic development, and due to potential roles within tumor cells. In particular, Nrp-1 is highly expressed in diverse tumor cell lines including human neoplasm and has been implications *in-vitro* and *in-vivo* during tumor growth and vascularization [19,20].

In the present study, we have successfully conjugated two peptides, therapeutic (p12) and targeted (CRGDK), on the surface of ultra-small *Au*NPs (2 nm) and characterized the conjugated nanocarrier. Ultra-small *Au*NPs can prove to be effective drug-based delivery systems for the treatment of breast cancer which overexpresses Nrp-1 receptor (Fig. 1).

2. Materials and methods

2.1. Chemicals

All the chemicals were of reagent grade and were used without further purification. Gold (III) chloride trihydrate (99.9%) were purchased Sigma–Aldrich (St. Louis, MO), (N-(3-dimethylaminopropyl)-N-ethylcarbodiimidehydrochloride, N-(2-mercaptopropionyl) glycine (>98%), $NaBH_4$ (98%), N-hydroxysuccinimide (>97%) and HEPES (2-[4-(2-hydroxyethyl) piperazin-1-yl] ethanesulfonic acid were purchased from Sigma–Aldrich (St. Louis, MO). The p12 peptide L-amino sequence reagents (NH_2-TSFAEYWNLLSP-NH_2) were purchased from BMJ, Technology, Ltd. (Beijing China), while CRGDK peptide was purchased from GL Biochem, (Shanghai, China). Clear-Amide Resin was purchased from Peptides International, Inc (Louisville, KY), and RPMI-1640 cell culture media was purchased from HyClone, Thermo (Beijing, China). Nrp-1(Neuropilin-1) antibody (ab81321 Rabbit-mAb) was obtained from Abcam (BioSci& Tech. LTD. Co, Beijing China), p53 (1C12 mouse mAb) and β-Actin (sc47778 mouse mAb) antibody from cell signaling (Shanghai, China), Goat-Anti-Mouse IgG (ZB-2305) was from Z.G.B, Biotec. Co. Ltd. (Beijing, China) and Goat-Anti-Rabbit IgG (Cat No. 31460) was from Thermo Scientific (Rockford, IL) All glass wares employed for NP preparation and storage was cleaned with aqua regia (HCl: HNO3, 3:1). House distilled water was further purified using a Milli-Q reagent grade water system. Millipore (18.2 MΩ cm) was used for the preparation of all aqueous solutions. Buffers were prepared according to standard laboratory procedure. All solutions used for nanoparticle preparation and conjugation were filtered through a 0.22 μm membrane filter (Whatman INC, Sanford, ME).

2.2. Instrumentations

The size of the *Au*NPs was analyzed via Transmission Electron Microscope (TEM) (Tecani-G2-20-S, TWIN, FEI, Hillsboro, OR). UV/VIS spectra and fluorescence measurements were carried out using a Lambda-950-PE (PerkinElmer, Waltham, MA). Charge distribution was studied using Zeta Potential (Zetasizer-MALVERN, Worcestershire, UK). Peptide was purified by HPLC (Waters-2796 Milford, MA) and ESI-MS mass spectra were recorded on a Bruker AMAZON ES Ion Trap spectrometer (Bruker Co, Bremen, Germany). MTT assay was measured with plate reader (TECAN-Infinite-M200, Männedorf, Switzerland). The concentration of gold was determined via ICP-MS (ELANDRC-PERKINELMER, Waltham, MA).

2.3. Synthesis of water soluble AuNPs (Au@tiopronin)

The 2 nm water soluble *Au*NPs were synthesized by procedure obtained from Murray et al. [21]. In this method, reactions preceded by adding Gold (III) chloride trihydrate (0.40 mmol) and N-(2-mercaptopropionyl) glycine (1.2 mmol) were co-dissolved in 21 ml of 6:1 methanol/acetic acid, giving a ruby-red solution. After continuous stirring, $NaBH_4$ (8 mmol), dissolved in 7.5 ml of H_2O, was used as a reductant and was added slowly with rapid stirring. After vigorous stirring for 2 h, a continuous black suspension was formed. The reaction temperature was then brought to normal or room temperature (RT). The black color resultant product was collected and concentrated under vacuum at 40 °C which was later dissolved in 20 ml of H_2O and dialyzed (Solarbio, MWCO = 8000–14,000) against Mill-Q water (3L) for more than 72 h with changes at every 10–12 h. The product was lyophilized and dried completely before using for further characterization studies.

2.4. Peptide synthesis and purification

Therapeutic peptide, p12, sequence (Table 1) was synthesized in our laboratory using *Fmoc* chemistry. In this method, clear resin was first swelled in DMF, then deprotected with 20% piperidine in DMF for 20 min, and washed thoroughly with DMF-DCM. 8 aliquots each of amino acids and HATU, and 16 aliquots of DIEA were added into DMF for mixing with the resin. The total volume is 2 ml and the reaction would last for 20 min at room temperature. After coupling, the resin was washed thoroughly against DMF-DCM, and then treated with 20% piperidine in DMF, washed completely and another amino acid was added to resin. These steps were repeated until all the amino acids were coupled onto the resin. After synthesis, peptide was cleaved from the resin using TFA cleavage cocktail for 2 h, filtered and precipitated in anhydrous diethyl ether, dried in vacuum and stored at −20 °C. The peptide was prepared in 0.1 mmol scale.

2.5. Functionalization of AuNPs with peptide CRGDK and p12 to obtain different derivatives of conjugations: Au@CRGDK, Au@p12, Au@p12 + CRGDK, Au@p12-CRGDK

In this method, reaction was carried out in HEPES 1X buffer (50 mM) at pH 6.5. 1 ml of *Au*@tiopronin (2 mg) solution was added in HEPES buffer. Then (N-(3-dimethylaminopropyl)-N-ethylcarbodiimide hydrochloride (EDC; 0.01 mM) and N-hydroxysuccinimide (NHS; 0.025 mM) were added to 5 ml of reaction buffer. The reaction proceeded for more than 30 min after which CRGDK (0.00043 mmol) and p12 peptide (0.00017 mmol) was added in two different reaction valves and thoroughly mixed with continuous stirring for more than 24 h. When the reaction mixture solution was loaded into dialysis membrane (MWCO = 8000–14,000) and placed in 3 L beaker of water and stirred slowly, by providing fresh water between 8 and 10 h time interval. *Au*@CRGDK and *Au*@p12 conjugation samples were collected from the dialysis membrane and lyophilized. The yield of dried product was calculated to be 1 mg.

For the conjugation of *Au*@p12-CRGDK and *Au*@p12 + CRGDK, the same procedure was followed as illustrated above. During the conjugation of *Au*@p12-CRGDK, both the peptides (p12 and CRGDK) were added together at the same time in the reaction mixture. In case of *Au*@p12 + CRGDK, the peptide p12 (therapeutic) was conjugated first. The second peptide, CRGDK (targeted) was conjugated after the first conjugated product has been dried or, alternatively, was added into the same reaction mixture after a gap of 24 h, following the conjugation of the first peptide. The dialysis process followed the same procedure for more than 24 h by providing 3 L of water with a time interval of 7–8 h.

2.6. Physicochemical properties of AuNPs and its conjugates

The *Au*NPs were suspended in Milli-Q water to achieve an appropriate level of scattering. The NPs were characterized using TEM, UV–Visible spectroscopy (UV–Vis) and size distribution of *Au*NPs were also measured to fit the Gaussian distribution and diameters of the NPs were calculated with mean size of 2 nm. After lyophilization process, *Au*NPs and its conjugates were dissolved in water and found

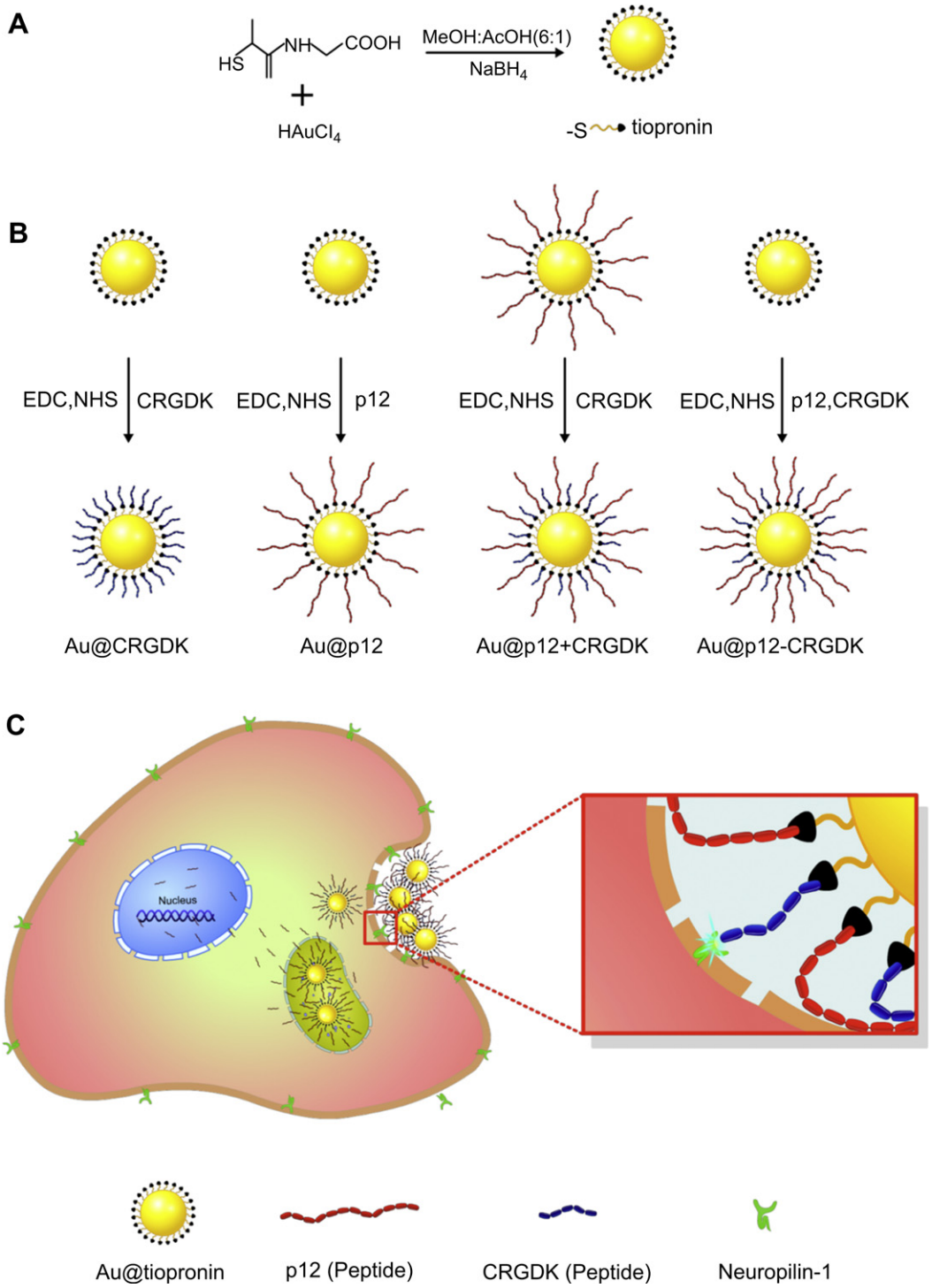

Fig. 1. Schematic illustration for the synthesis of *Au*@tiopronin and functionalization with peptides for cancer treatment: (A) Synthesis of *Au*@tiopronin. (B) *Au*NPs functionalized with two different types of peptides, therapeutic (p12) and targeted (CRGDK). (C) Interaction between the receptor and targeted ligand enhances intracellular entry and increases response to intracellular release of therapeutic peptide into the cells.

to be stable at 4 °C. However, slight aggregation of nanoparticles appears in the conjugated solution following storage of more than two weeks.

2.7. Agarose gel electrophoresis

The gel electrophoresis of 2 nm *Au*NPs and its conjugated samples was done by modifying the method of Xu et al. [22]. The 2 nm *Au*NPs and its conjugated samples were loaded into the wells of a 2% agarose gel. The samples were prepared by adding 12–15 μl Glycerin to 84 μl of sample, from which 20 μl sample was added into wells. The electrophoresis was run under 115 V in 1X TAE buffer. The separated bands of the conjugated sample and control sample (*Au*NPs without any peptide) bands were measured in bright field gel counter.

2.8. Quantification of peptides conjugated to AuNPs surfaces

The amount of peptide loaded onto the surface of *Au*NPs was quantified by BCA (Bicinchoninic acid) method. In this experiment, *Au*NPs in the form of diluted sample (200 μg/ml) was kept as blank (negative control) and free peptide was kept

as positive control (200 μg/ml). Concentration of *Au*NPs in the conjugated samples, *Au*@CRGDK and *Au*@p12, were similar to that of blank and was measured by BCA assay. The values of optical density (O.D.) at 570 nm were plotted on a standard curve, and the amount of peptide was calculated in the conjugated sample using following formula (Eq. (1)). The *Au*NPs did not affect the O.D. value during the assay. *Au*@CRGDK showed 90% conjugation of peptide, while *Au*@p12 revealed 65% conjugation efficiency.

$$\begin{gathered}\text{Amount of peptide on } Au\text{NPs Surface} = [\text{OD}_{570} \text{ of } Au\text{@peptide} - \text{OD}_{570} \text{ of background}] - \\ [\text{OD}_{570} \text{ of control} - \text{OD}_{570} \text{ of background}] \\ Au\text{@peptide} - Au\text{@tiopronin} = \text{Amount of peptide} \\ Y = A + B^{*}X \text{ [from standard graph]} \\ X = (Y - A)/B \end{gathered} \quad (1)$$

Y = Actual OD_{570} of Sample; A is a constant and B is a coefficient both obtained from linear fitting; X = μg/ml was calculated by putting the value of A and B in equation.

2.9. Cell culture and cytotoxicity assay

MDA-MB-231 and MCF-7S human breast adenocarcinoma cells, purchased from the Chinese Academy of Medical Sciences & Peking Union Medical College, Beijing, China, were grown in RPMI-1640 and DMEM (LG) medium supplemented with 10% fetal calf serum (FCS), 2 mM L-glutamine, penicillin (100 U/mL), and streptomycin (100 μg/mL). All cell lines were maintained at 37 °C in an atmosphere of 5% CO_2.

2.10. Treatment of cells with AuNPs and its conjugates

MDA-MB-321 and MCF-7S cells were seeded in 96-well plates at a density of 5×10^4 cells/well/100 μl. Cells were first cultured for 24 h and then treated with free peptide, unconjugated *Au*NP, and its conjugates at various concentrations (1–100 μg/ml or 4–400 nM) for 24 h or, in case of MDA-MB-321 cells, treated for another 24h. Cell viability was determined using MTT assay. 100 μl MTT solutions (0.5 mg/ml) was added to each well following treatment time, and incubated for 4 h at 37 °C. The MTT solution was replaced with 100 ml DMSO. The absorbance at 570 nm for each well was measured on an Automated Microplate Reader (TECAN-Infinite-M200). Viability of the non-treated control cells was calculated to be 100%. The Cell viability (%) was calculated using the following formula (Eq. (2)).

$$\begin{gathered}\text{Cell lethality (\%)} = [1 - (\text{OD}_{570} \text{ nm of sample} - \text{OD of blank sample})]/ \\ [(\text{OD}_{570} \text{ nm control} - \text{OD}_{570} \text{ nm blank})] \times 100\% \end{gathered} \quad (2)$$

where "sample" and "control" mean the cells with and without treatment with *Au*NPs and its conjugates, respectively.

2.11. Quantification of cellular uptake of AuNPs

The cells were plated in 6-well culture plates at 5×10^5 cells per well and allowed to grow until 80% confluency. The cells were then given a dose of 50 μg/ml (200 nM) *Au*NP and its conjugated samples, and then incubated for 24 h. Later, cells were washed 2–3 times with 1X PBS buffer to remove any excessive or unbound NPs from the cells' outer surface, and digested with aqua regia (HCl:HNO_3, 3:1). The results were analyzed using ICP-MS and amounts of *Au*NPs were calculated based on the concentration of *Au* found in the sample [23].

2.12. Western blot analysis of cancer cells after treatment

Cells obtained after treatment were washed twice with ice cold 1X PBS and resuspended by scrubbing in cold conditions with a lysis buffer containing 0.5 mM PMSF. The homogenized cells were centrifuged at 12,000 g for 15 min, and supernatant was collected for analysis. The total protein concentration was determined by spectrophotometer. Samples of 20 μg/20 μl of total protein per lane were separated on 10 and 8% sodium dodecyl sulfate-polyacrylamide gel (SDS-PAGE). The 10% gel was used for determination of p53 protein and 8% for Nrp-1. The resultant proteins were blotted onto 0.2 mm PVDF membrane. The membrane was incubated in 5% skimmed milk with 0.1% Tween-20 in TBST for 3 h at room temperature to avoid unspecific binding. The membrane was then incubated with p53 primary mouse monoclonal antibody diluted 1:1000 (v/v) overnight at 4 °C in TBS with 2% milk and peroxidase-conjugated goat-anti-mouse IgG diluted 1:5000 (v/v) for 1.5 h at room temperature in TBST. Similarly, 8% gel was transferred to membrane and incubated with Nrp-1 rabbit monoclonal antibody dilution 1/1000 (v/v) and peroxidase-conjugated goat-anti-rabbit dilution 1:5000 (v/v). As internal standard for the proteins, the membrane was also incubated with β-Actin mouse monoclonal antibody dilution 1:200 (v/v) and goat-anti-mouse peroxidase-conjugated goat-anti-mouse IgG (1:5000 (v/v) dilutions). The membranes were exposed to Kodak X-Omat film using ECL reagent for various times and the densitometric intensities of protein bands were determined.

2.13. Statistical analysis

Standard statistical methods were used. Parametric methods (*t*-test) were used for evaluation and significance tests were considered at P less than 0.05 (2-tailed tests). Data are presented as means (SD) of at least 3 individual experiments.

3. Result

3.1. Synthesis and characterizations of AuNPs

The NPs were synthesized using the procedure developed by Murray et al. [21]. Initially, the reaction was carried out in methanol/acetic (6:1) acid mixture (Fig. 1A). The addition of H*Au*Cl_4 and Tiopronin gave a ruby-red color solution. After the addition of reductant ($NaBH_4$), the color of the solution changed from ruby-red to dark brown. The whole reaction was preceded for 2 h after which the solvent was removed under vacuum dryer at 40 °C. The product was purified by dialysis process and characterization study was done by TEM, UV–Vis, and Zeta potential. The molecular weights of the particles were determined in accordance with the ICP-MS results.

Moreover, *Au*NPs (*Au*@tiopronin) were very easily soluble in water and stable in physiological conditions, NPs did not appear to be aggregated. TEM analysis revealed *Au*NPs with a very small core size of 2 nm with uniform dispersion (Fig. 2A). The UV–visible absorbance measurement of *Au*NPs showed surface plasmon peak bands detectable at 506 nm (Fig. 2C) but the peak was not so obvious. It is well-known that in the case of smaller NPs, surface plasmon bands are non-detectable [24]. The Zeta potential studies of *Au*NPs in water showed negatively charge to be −41.2 (Table. S1). The sizes of *Au*NPs were measured to fit the Gaussian distribution with mean size of 2 nm (Fig. 2B) and diameters were calculated by counting more than 1000 of *Au*NPs.

3.2. Peptide preparation and conjugation with AuNPs for physicochemical characterization

The crude therapeutic peptide was purified by RP-HPLC using Waters *XBridge* C18 column. After purification, the analytical HPLC and ESI-MS data (Fig. 3A and B) suggests the molecular weight of peptide to be 1426.6, which was similar to the calculated molecular weight with a purity of 99%.

With an aim of developing *Au*NPs conjugate with therapeutic and target peptide, Nrp-1 receptor was selectively targeted to enhanced delivery of therapeutic molecules and achieve higher toxic effects on cancerous cells, we have attempted the functionalization of *Au*NPs with the two different peptides using two different procedures. The functionalization of *Au*@tiopronin with CRGDK peptide was prepared according to the procedure of Fuente et al. [25]. The presence of free carboxyl group of tiopronin helps in the conjugation of peptide with the amino terminal. The reaction was catalyzed by adding EDC which helped in the formation of more amide bond between the *Au*NPs and peptide. At the same time, NHS was added in the reaction mixture to improve the efficacy of amide bond to protect it from hydrolysis (hydrolysis resistance intermediate). In parallel, same procedure was repeated separately for the conjugation of p12 peptide with *Au*NPs to get *Au*@p12. The quantification of peptide onto the *Au*NPs surface was studied by BCA method, whereby the amount of the peptide present on the gold surface was calculated using (Eq. (1)) to obtain values in μg/ml and finally the amount of peptide was converted into percentage. Our quantification studies show that 90% of the peptide was conjugated in the case of *Au*@CRGDK and 65% of peptide was conjugated in case of *Au*@p12.

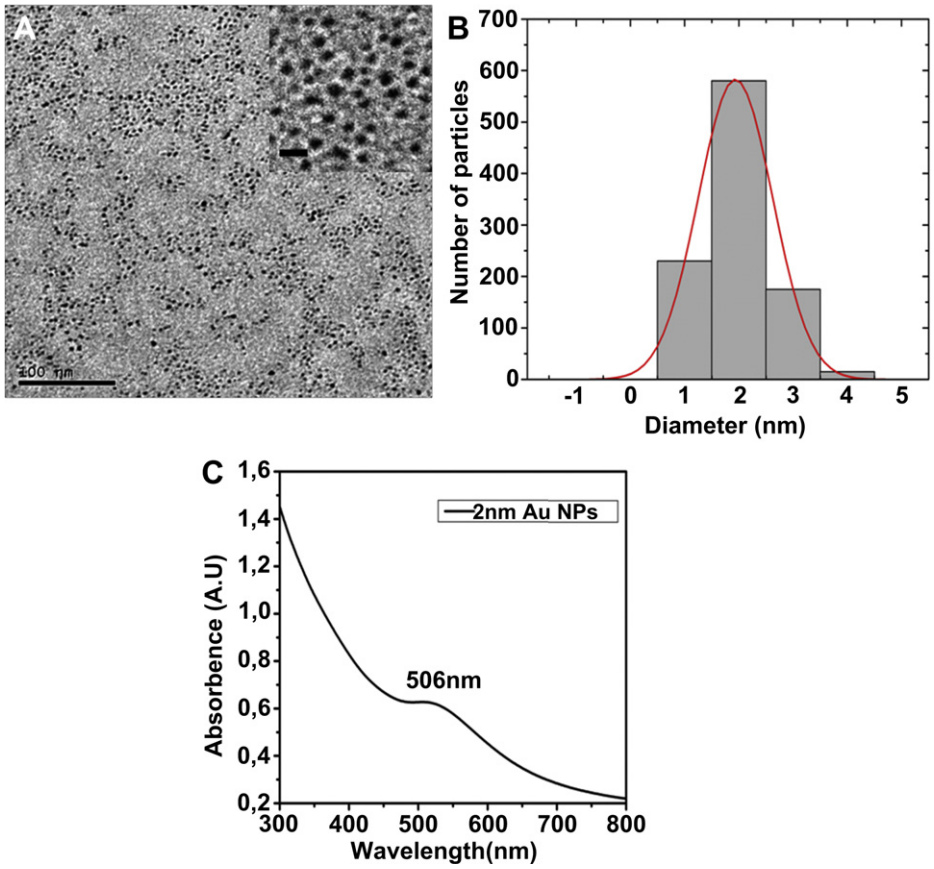

Fig. 2. Characterization of *Au*NPs: (A) Typical image TEM of *Au*NPs in H_2O (Scale bar = 100 nm) Upper right smaller nanoparticles products, an insert showing almost equal size distribution (scale bar = 5 nm). (B) Histogram depicting size of 1000 particles, fitted to Gaussian distribution with mean size 2 nm. (C) UV–Vis absorbance of *Au*NPs at 506 nm was detected but not obvious.

During the conjugation process involving both p12 and CRGDK, we observed that the saturation level of CRGDK onto the *Au*NPs was less when combined with p12 at the same time (might be due to competition between the two peptides), which, henceforth has been designated as *Au*@p12-CRGDK (the negative sign indicates low saturation level of CRGDK). On the other hand, the *Au*NPs containing p12 and CRGDK at fully saturated level has been designated as *Au*@p12 + CRGDK (positive sign indicates more saturation of CRGDK). In case of *Au*@p12 + CRGDK the target peptide was added after the conjugation of *Au*@p12, which shows higher toxicity compared to all other conjugations. No aggregation was observed during the conjugation process. The resultant *Au*NP-

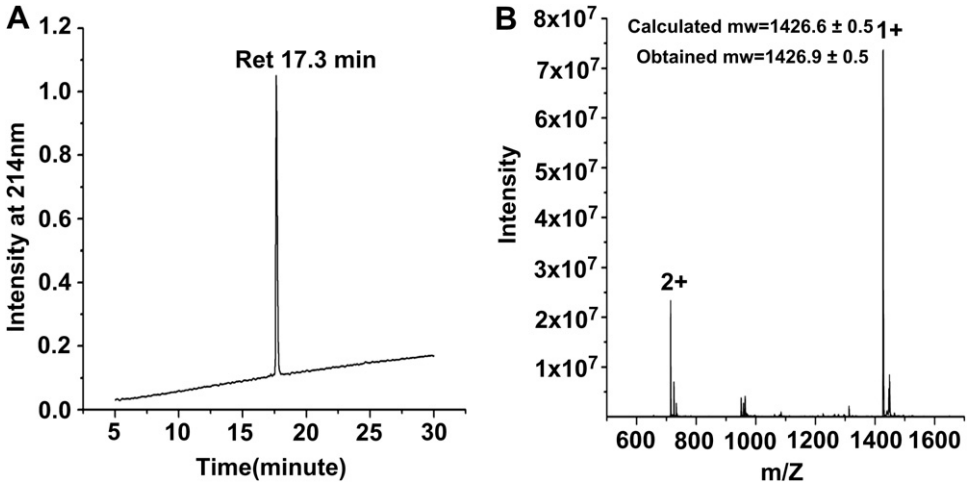

Fig. 3. Characterization of PMI (p12) peptide: (A) 214 nm HPLC trace. Solvent A: H_2O with 0.1% formic acid; Solvent B: Acetonitrile with 0.1% formic acid. RP-HPLC was carried out using linear gradient elution from 5% B to 65% at 1 ml/min for 30 min at 40°C. (B) ESI-MS data was collected through direct injection with the targeting molecular mass 1500 and ion charge was set to positive.

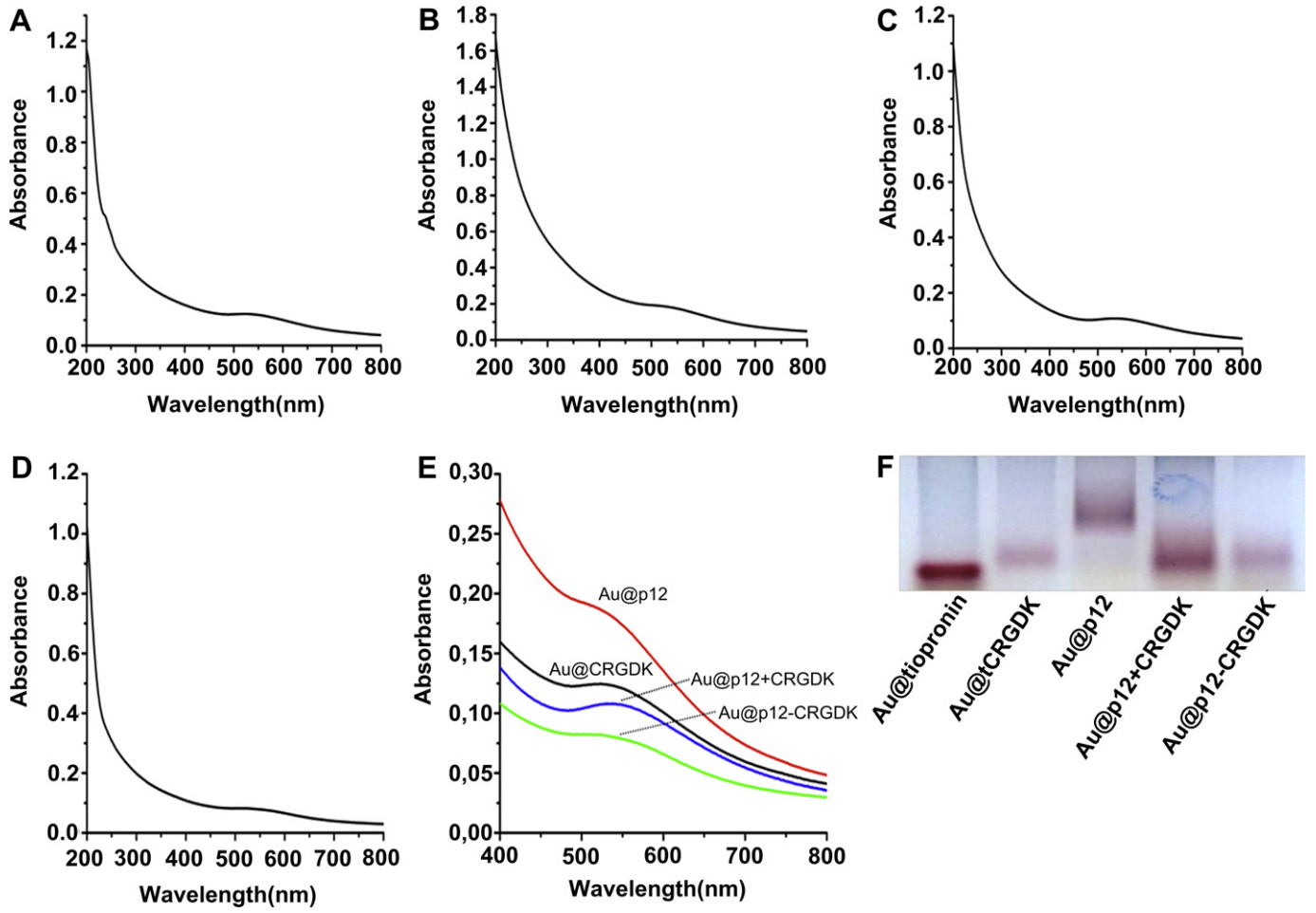

Fig. 4. Characterization of *Au*NPs before and after conjugation with peptide by UV–Vis spectra and electrophoresis measurement: (A) *Au*@CRGDK. (B) *Au*@p12. (C) *Au*@p12+CRGDK. (D) *Au*@p12-CRGDK. UV-Vis absorbance measurement of all conjugated samples was measured and compared to free *Au*@tiopronin. (E) There was no significant plasmon band peak because of the small size but the different absorbance in all the conjugated sample variations were observed when all the four conjugated samples were depicted in one graph. (F) Agarose gel electrophoresis was used for qualitative measurement of the presence of peptide on the surface of *Au*NPs, whereby, differences in mobility of *Au*NPs after conjugation with peptide were observed. The gel image provided the presence of peptide onto the *Au*NPs surface with smear. All the lanes were loaded with equal volume of conjugated sample (1 mg/ml) except *Au*NPs@tiopronin (2 mg/ml to indicate for identification).

conjugates were characterized by UV–Vis (Fig. 4A–D, and E), Zeta potential (Fig. S1 and ST1 see Supplementary data), and agarose gel electrophoresis method (Fig. 4F). During the UV–Visible absorbance in all the *Au*NPs conjugated samples, the surface plasmon peak band was non-detectable due to the small size but the differences in the peak variation [26] was observed in each conjugated sample compared to the surface plasmon peak of unconjugated *Au*NPs (Fig. 2C). The significant change in charge distribution was observed in case of all conjugated samples (Fig. S2 and S3-see Supplementary data) when compared to unconjugated *Au*NPs charge which itself showed negative charge of −41.2. Upon conjugation with CRGDK (hydrophilic peptide), the charge shifted to positive direction (−24.1) indicating the presence of CRGDK on *Au*NPs' surfaces. In the case of p12 (hydrophobic) peptide, the charge of conjugated sample was −37.5 indicating the presence of p12 onto the *Au*NPs surface. Similarly, the charge of *Au*@p12 + CRGDK again shifted to the positive direction (−23.7) which was almost similar to *Au*@CRGDK. However, in the case of *Au*@p12-CRGDK, a more significant shift in charge distribution was observed (−6.70) which might be due to the unbalance of charge between the two peptides.

Herein, we have also attempted to confirm the conjugation of functionalized *Au*NPs through agarose gel electrophoresis (Fig. 4F) a smear was observed with slow mobility in all other conjugated samples compared to *Au*@tiopronin (unbound *Au*NPs), indicating the presence of peptide onto the *Au*NPs surface [6]. After conjugation, all the resultant products were lyophilized and dried completely under vacuum conditions and dissolved in water for further experimental procedures.

3.3. Cytotoxicity of AuNPs and its conjugates

The cytotoxic effects of *Au*@tiopronin (unconjugated *Au*NPs), free peptides and conjugated *Au*NPs (namely *Au*@CRGDK, *Au*@p12, *Au*@p12 + CRGDK and *Au*@p12-CRGDK) against cultured MDA-MB-321 cells were evaluated using the MTT assay [27]. MDA-MB-321 is a type of breast cancer cell line which overexpresses Nrp-1 receptor. It showed no toxic effect on the cells when treated with unbound *Au*NPs and free peptides (100 ug/ml = 0.00018 mM). In the case of p12 peptide, a higher concentration (50 μM) of free peptides did not show any toxicity to the cells as the peptide itself is unable to enter inside the cells [28]. However, after the conjugation of peptide with *Au*NPs, cell viability decreased. The significant difference in viability was observed in the conjugated samples (Fig. 5A). *Au*@CRGDK also shows toxicity to cells around 25–30%, *Au*@p12 show higher toxicity (40–50%) than the *Au*@CRGDK due to

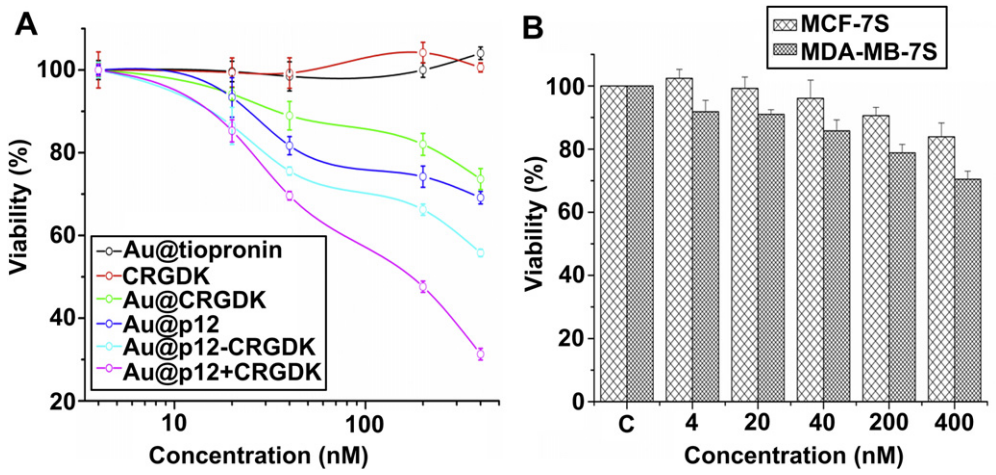

Fig. 5. Cytotoxicity effects of all conjugate samples measured by MTT assay: (A) Cell viability was checked after 24 h treatment with unconjugated *Au*NPs, Au@CRGDK and all other conjugated samples (dosage 4–400 nM). Unconjugated *Au*NPs and free peptides themselves have no cytotoxic effects, but after conjugation, the *Au*NPs revealed synergistic effects which were evident in all conjugate samples. The peptide PMI (p12) (50 μM) itself had no effects on cell viability (data not shown), but the *Au*@p12 showed significant cytotoxic effects which was maximal in the *Au*@p12+CRGDK conjugation. (B) Comparison of cell viability on MCF-7S and MDA-MB-321 cells incubated with *Au*@CRGDK with similar dosage in both cell lines, wherein MCF-7S showed lower effects than MDA-MB-321.

the therapeutic effects of p12. The highest toxicity effects was observed in case of *Au*@p12 + CRGDK which was around 70%, revealing that the amount of CRGDK peptide conjugated on *Au*NPs surface was comparatively more resulting in increased targeted delivery compared to *Au*@p12. However, in the case of *Au*@p12-CRGDK nanoparticles showed toxicity lower than that of *Au*@p12 + CRGDK which indicated that the amount of targeted peptide loaded on the *Au*NPs was comparatively less than that of

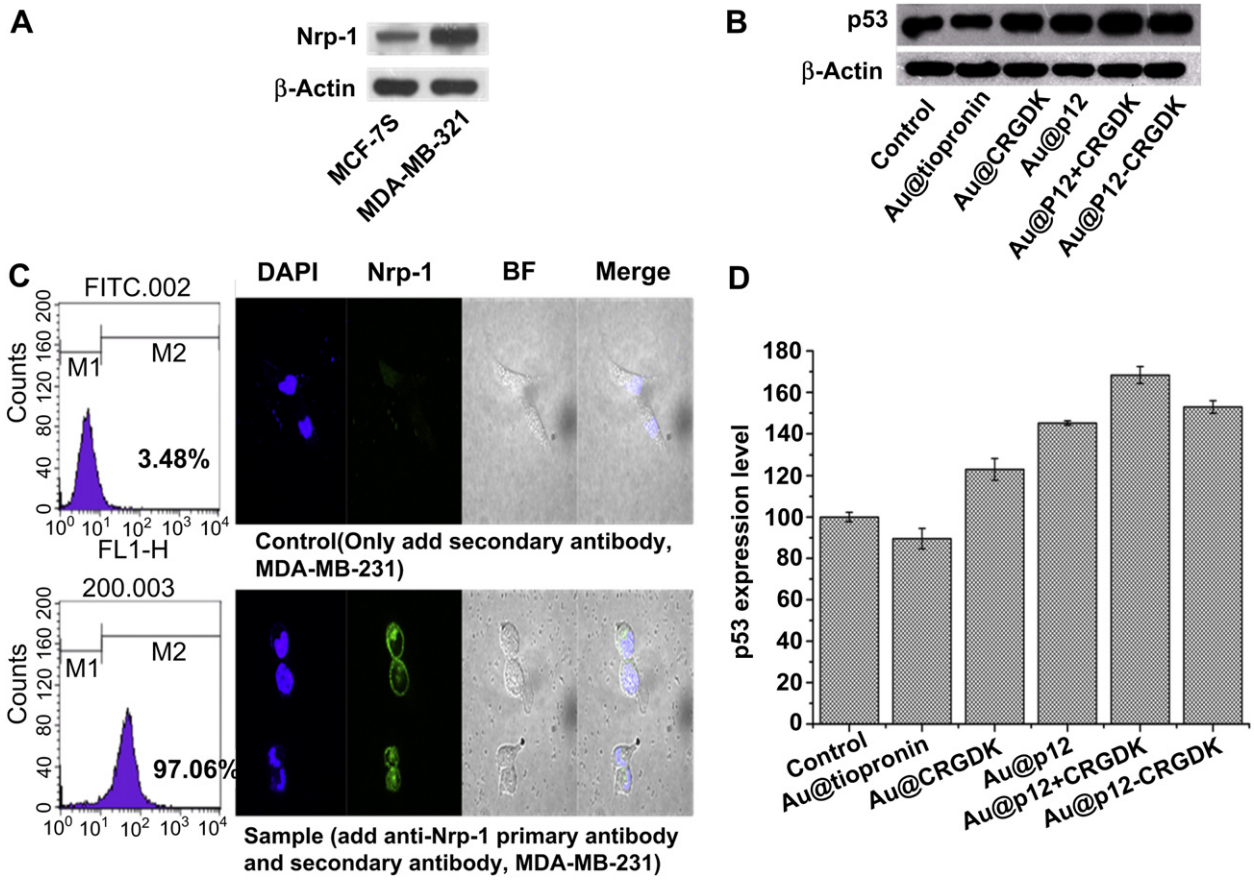

Fig. 6. Protein expression profile: Nrp-1 expression in MCF-7S and MDA-MB-321 cell lines (A) and p53 expression in MDA-MB-321 cells line (B) by western blot analysis. p53 expression was measured in MDA-MB-321 cells after treatment of AuNPs with various conjugations. Total protein/lane (20 μg/ml) was separated by 8% and 10% gel and transferred to a PVDF membrane and treated using two different specific primary antibodies, filter washed, and than immunoblotted with peroxidase-conjugated secondary antibody. (C) Confocal study of Nrp-1 expression in MDA–MB-321 cell line using FITC labeled Nrp-1 antibody. (D) Relative p53 expression levels were normalized to the protein levels of β-actin. Data is shown as mean ± SD ($n = 3$).

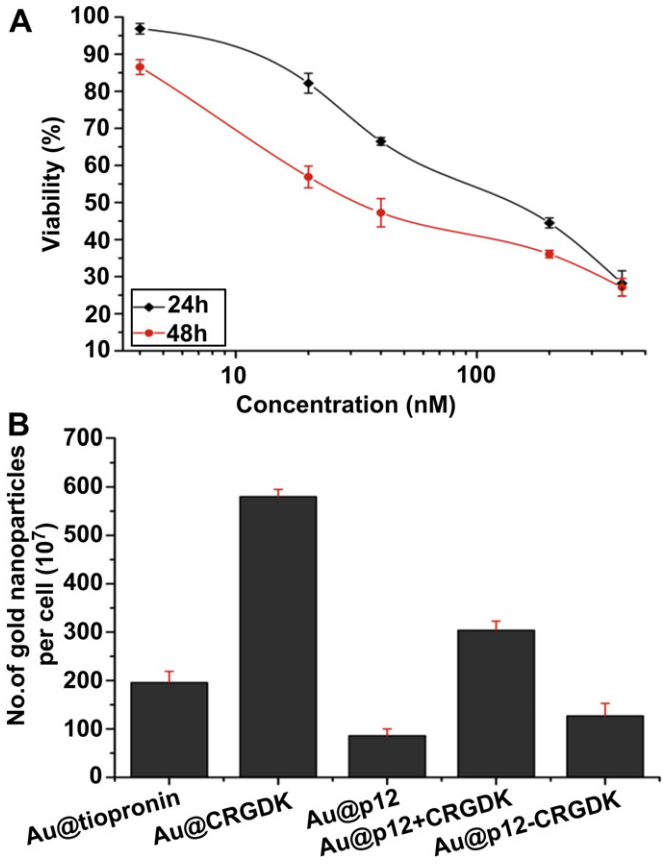

Fig. 7. Cytotoxicity and cellular uptake of *Au*NPs and all conjugates: (A) Cytotoxicity of *Au*@p12+CRGDK on MDA-MB-321 cell line at two different time interval (24 h, 48 h), wherein significant decrease in cell viability was observed. (B) Cellular uptake of *Au*NPs after 24 h treatment with unconjugated as well as conjugated *Au*NPs, uptake efficiency was directly proportional to the nature of functionalization of *Au*NPs.

Au@p12 + CRGDK. So, we selected *Au*@p12 + CRGDK is an effective candidate among the other conjugated nanoparticles. After 24 h treatment with *Au*@p12 + CRGDK, the IC_{50} value was measured to be 141 nM while further treatment of 24h resulted in decrease of the IC_{50} value up to 4-fold (32 nM) (Fig. 7A).

We have also analyzed the effects of *Au*NPs conjugated targeted peptide (*Au*@CRGDK) on MCF-7S cell line with dosage same to MDA-MB-321 cells, and found that MCF-7S has comparatively lower toxicity than MDA-MB-321 cells (Fig. 5B). The results seemed obvious as MCF-7S cell line has lower expression level of Nrp-1 receptor, thus indicating target specificity of the conjugated peptide.

3.4. Intracellular uptake of AuNPs measured with ICP-MS

The cellular uptake of *Au*NPs and its conjugated samples was determined by ICP-MS [23], with Nrp-1 receptor positive MDA-MB-321 cell line. In all the conjugated nanoparticles, significant difference of *Au*NPs uptake was observed (Fig. 7). The Nrp-1 receptor on the cells surface can greatly affect the rate of cellular uptake for the nanoconjugates. We measured the cellular uptake for each nanoconjugate to ensure that the difference in uptake of conjugated *Au*NPs was not due to *Au*NPs itself but because of the presence of ligand receptor interaction. Higher uptake level was found in the case of *Au*@CRGDK and very low uptake level was observed in the case of *Au*@p12 because of the absence of CRGDK. In the p12 and CRGDK functionalized nanoparticles, there was higher uptake of *Au*@p12 + CRGDK nanoparticles than that of *Au*@p12-CRGDK nanoparticles. The difference might be influenced by the variations in the conjugation level of CRGDK on *Au*NPs surface.

3.5. Nrp-1 expression and functional properties of p12 (PMI) shown as p53-dependent

Neuropilin-1 (Nrp-1) is a key receptor expressed by various cancer cell lines and plays an important role in growth and progression of cancer. To further investigate our results, we checked the Nrp-1 expression in MCF-7S and MDA-MB-321 cells lines by Western-blotting (Fig. 6A) and confocal microscopic imaging (Fig. 6C) to confirm the presence of receptors. After treatment with primary and secondary antibody, we found that MCF-7S has lower level of Nrp-1 expression as compared to MDA-MB-321 cells line.

The interaction of p53 inhibitor with oncogenic proteins, MDM2 and MDMX, is of therapeutic importance in cancer treatment. Previous reports suggest that the potent inhibitor is active at low nanomolar concentrations against the MDM2 and MDMX complex [15]. Binding affinity of p12 (PMI) to the complex activates the transcriptional activity of p53 which results in overexpression of p53 protein [28]. To further investigate the intracellular mechanism of PMI, we analyzed the expression of p53 protein in MDA-MB-321 cell lines by Western-blotting techniques. After 24 h treatment with *Au*NPs and all conjugated sample with dosage similar to the MTT assay (400 nM), we found that induction of p53 protein expression was increased in all treatments with conjugated nanoparticles (Fig. 6B and D). The consequence of p53 expression was similar with the cell viability results. The levels of p53 protein expression were higher in case of *Au*@p12 + CRGDK compared to all other conjugates which is due to the presence of more p12 and CRGDK onto the *Au*NP's surface resulting in increased delivery of p12 peptide with *Au*NPs inside cells.

Earlier works reported by Chan and co-workers [6] demonstrated that *Au*NP itself downregulated the expression of various p53 signaling protein such as caspase-3, capase-9, p27, etc. and similar results were also observed in our case wherein cells treated with unbound *Au*NPs showed downregulation of p53 protein expression. The overall results strongly support that PMI plays a significant role in inhibition of cell growth in breast cancer by reacting with the p53 signaling pathway.

4. Discussions

*Au*NPs with different sizes and characteristic properties were developed and extensively analyzed in recent years for various biomedical applications [29,30]. Among *Au*NPs with size over 10 nm, thiol-stabilized *Au*NPs are particularly attractive nanomaterials for various applications such as nanoelectronics, catalysis, optics, chemical and biological sensing, and the recent most potential application in nanomedicine [31]. The stabilizing molecules, besides preventing the formation of aggregation, are also essential for controlling the chemical reactions and subsequently responsible for the well dispersed size and its uniformity. Tiopronin (N-(2-mercaptoproionyl) glycine) is a pharmaceutical drug used for the treatment of cystinuria and rheumatoid arthritis, and its basic biocompatibility is quite well established. It is employed to synthesize ultra-small (2 nm) *Au*NPs as reduction agents in this study.

Au@tiopronin has been previously used in materials science although it has not been explored widely in biological field. To control the exact size of ultra-small gold nanoparticles is very hard during synthesis process. However, the stability of *Au*NPs in physiological environment is an important factor for targeted delivery due to their small size, large surface area to mass ratio, high surface reactivity, simple straight forward synthesis, high water solubility, their biocompatibility and ease of surface functionalization. Recently, several groups have reported the use of *Au*NPs for the successful delivery of drugs like doxorubicin for overcoming drug

resistance in cancer [32] as well as peptide functionalized *Au*NPs for targeting tumor [33]. The free carboxyl group presented in *Au*@tiopronin strongly participates in covalent coupling with various biological molecules by cross-linking to reactive amino acids [34]. An ideal therapeutic approach would be to deliver multiple drugs specifically to the primary tumors, as well as at the site of metastasis and its microenvironment while simultaneously monitoring the prognosis through non-invasive approaches. In cancer therapy, targeted delivery in a localized way is one of the key challenges. *Au*NPs have the potential to play a significant role to achieve such goals. It is anticipated that NP-mediated targeted delivery of drugs might significantly reduce the dosage of anti-cancer drugs with better specificity, enhanced efficacy and lower toxicities. Therefore, we have developed an *Au*NP-based targeted delivery system (DDS) with size about 2 nm for *in-vitro* therapeutic applications in breast cancer cells.

In our study, we have described the synthesis and characterization of a therapeutic (p12) and targeted peptide (CRGDK) functionalized onto ultra-small *Au*NPs' surface for the treatment of cancer. PMI (p12) as the therapeutic molecule was demonstrated as an effective molecule for inhibiting the growth of cancer cells in a p53-dependent manner through manifold interactions with the MDMX and MDM2 complex. Neuropilin-1 is thought to act as a co-receptor for VEGF by forming complexes. The viability measurement demonstrated that Nrp-1-targeted ligands on the surface of *Au*NPs played an important role in enhancing the cytotoxic effect by binding the CRGDK molecules with the overexpressed receptor located on the surfaces of MDA-MB-321 cells and subsequently increasing their intracellular uptake as a result of receptor-mediated endocytosis. The presence of Nrp-1 receptor on the cell surface may increase the binding affinity between CRGDK-conjugated *Au*NPs and Nrp-1 cell receptors through competitive interactions.

To investigate the role of Nrp-1 in cellular uptake of *Au*NPs, MCF-7S cell line with low level of Nrp-1 receptor expression on the cells surface was incubated with *Au*@CRGDK (concentration same as in MDA-MB-321 cell line). The toxicity effects of *Au*@CRGDK on MCF-7S cells were lower as compared to MDA-MB-321 cell line (Fig. 6A). Similar phenomenon was also observed in case of *Au*@p12-CRGDK-conjugated nanoparticles; cell toxicity after 24 h treatment with *Au*@p12-CRGDK was higher than that of *Au*@p12 but was lower than *Au*@p12 + CRGDK-conjugated nanoparticle in that amount of CRGDK peptide conjugated to the *Au*@p12 + CRGDK was higher than that of *Au*@p12-CRGDK. These results confirm that CRGDK molecules increase the efficacy for delivery of *Au*NPs conjugated therapeutic molecules by competitive binding to the Nrp-1 receptors on the cancer cell surface.

We originally hypothesized that the ligand CRGDK would cause the greater endocytosis of NPs by the cells and would subsequently show highest cellular uptake and cytotoxicity. The cellular uptake studies indicated that unconjugated *Au*NPs as well as *Au*@p12 had the lowest uptake level by cells compared to receptor-targeted conjugation systems. In this case, CRGDK involved in competitive binding to the Nrp-1 receptors on the cancer cell surface, thus, helping in successful delivery of the therapeutic peptide (p12) into the cells.

The intracellular activity of therapeutic peptide was measured through the p53 expression. *Au*@p12 + CRGDK nanoparticles played a significant role in interacting with the MDMX and MDM2 complex, which results in overexpression of p53 protein in cells after 24 h treatment. The level of p53 expression was higher in all conjugated nanoparticles compared to control *Au*NPs. p53 protein was found with high expression in *Au*@p12 + CRGDK NPs treated cells due to higher uptake of p12 molecules into the cells aided by the CRGDK molecules.

5. Conclusion

The present work developed a gold-based nanocarrier decorated with therapeutic as well as receptor-targeted peptide to study the bio-effects of *Au* conjugated nanoparticles on breast cancer cells. Moreover, the small *Au*NPs (2 nm) was successfully synthesized, functionalized and characterized to further help in successful delivery of both peptides into the cells through interactions with Nrp-1 receptor. The uptake of p12 was significantly facilitated by cancer cells due to Nrp-1 mediated recognition and internalization. *Au*@p12 + CRGDK exhibited stronger *in-vitro* anti-cancer activity than other conjugates. These results indicated that the *Au*NPs functionalized with therapeutic and targeted peptides could be a promising anti-cancer nanosystem to achieve better efficacy for therapeutic molecules. This type of drug delivery systems (DDSs) can be developed to carry with one or more drugs and multiple targeting agents as theranostic nanoparticles for imaging and therapeutic usages and also for multiple applications.

Acknowledgments

This work was supported in part by Chinese Natural Science Foundation project (No. 30970784 and 81171455), National Key Basic Research Program of China (2009CB930200), Chinese Academy of Sciences (CAS) "Hundred Talents Program" (07165111ZX) and CAS Knowledge Innovation Program.

Appendix. Supplementary material

Supplementary material related to this article can be found online at doi:10.1016/j.biomaterials.2011.10.058.

References

[1] Paciotti GF, Kingston DGI, Tamarkin L. Colloidal gold nanoparticles: a novel nanoparticle platform for developing multifunctional tumor-targeted drug delivery vectors. Drug Dev Res 2006;67:47–54.
[2] Rotello VM, Ghosh P, Han G, De M, Kim CK. Gold nanoparticles in delivery applications. Adv Drug Deliver Rev 2008;60:1307–15.
[3] Rotello VM, Duncan B, Kim C. Gold nanoparticle platforms as drug and biomacromolecule delivery systems. J Control Release 2010;148:122–7.
[4] Connor EE, Mwamuka J, Gole A, Murphy CJ, Wyatt MD. Gold nanoparticles are taken up by human cells but do not cause acute cytotoxicity. Small 2005;1:325–7.
[5] Niidome T, Pissuwan D, Cortie MB. The forthcoming applications of gold nanoparticles in drug and gene delivery systems. J Control Release 2011;149:65–71.
[6] Chan WCW, Jiang W, Kim BYS, Rutka JT. Nanoparticle mediated cellular response is size-dependent. Nat Nanotechnol 2008;3:145–50.
[7] Zhang SL, Li J, Lykotrafitis G, Bao G, Suresh S. Size-dependent endocytosis of nanoparticles. Adv Mater 2009;21:419–24.
[8] Shortkroff S, Turell M, Rice K, Thornhill TS. Cellular response to nanoparticles. Mater Res Soc Symp P 2002;704:375–80.
[9] Dasgupta AK, Patra HK, Banerjee S, Chaudhuri U, Lahiri P. Cell selective response to gold nanoparticles. Nanomed Nanotechnol 2007;3:111–9.
[10] Tamarkin L, Libutti SK, Paciotti GF, Byrnes AA, Alexander HR, Gannon WE, et al. Phase I and pharmacokinetic studies of CYT-6091, a novel PEGylated colloidal gold-rhTNF nanomedicine. Clin Cancer Res 2010;16:6139–49.
[11] Bischof JC, Goel R, Shah N, Visaria R, Paciotti GF. Biodistribution of TNF-alpha-coated gold nanoparticles in an in vivo model system. Nanomedicine-UK 2009;4:401–10.
[12] Kim C, Agasti SS, Zhu ZJ, Isaacs L, Rotello VM. Recognition-mediated activation of therapeutic gold nanoparticles inside living cells. Nat Chem 2010;2:962–6.
[13] Torchilin VP. Cell penetrating peptide modified pharmaceutical nanocarriers for intracellular drug and gene delivery. Biopolymers 2008;90:604–10.
[14] Giljohann DA, Seferos DS, Daniel WL, Massich MD, Patel PC, Mirkin CA. Gold nanoparticles for biology and medicine. Angew Chem Int Ed 2010;49:3280–94.
[15] Lu W, Pazgiera M, Liu M, Zou GZ, Yuan WR, Li CQ, et al. Structural basis for high-affinity peptide inhibition of p53 interactions with MDM2 and MDMX. P Natl Acad Sci USA 2009;106:4665–70.
[16] Khvax Lu. Live or let die: the cells response to p53. Nat Rev Cancer 2002;2:594–604.
[17] Momand J, Wu HH, Dasgupta G. MDM2-master regulator of the p53 tumor suppressor protein. Gene 2000;242:15–29.

[18] Banerjee S, Stephenson JM, Saxena NK, Cherian R, Banerjee SK. Neuropilin-1 is differentially expressed in myoepithelial cells and vascular smooth muscle cells in preneoplastic and neoplastic human breast: a possible marker for the progression of breast cancer. Int J Cancer 2002;101:409–14.
[19] Klagsbrun M, Bielenberg DR, Pettaway CA, Takashima S. Neuropilins in neoplasms: expression, regulation, and function. Exp Cell Res 2006;312:584–93.
[20] Ruoslahti E, Sugahara KN, Teesalu T, Karmali PP, Kotamraju VR, Agemy L, et al. Tissue-penetrating delivery of compounds and nanoparticles into tumors. Cancer Cell 2009;16:510–20.
[21] Murray RW, Templeton AC, Chen SW, Gross SM. Water-soluble, isolable gold clusters protected by tiopronin and coenzyme a monolayers. Langmuir 1999; 15:66–76.
[22] Scrivens WA, Xu XY, Caswell KK, Tucker E, Kabisatpathy S, Brodhacker KL. Size and shape separation of gold nanoparticles with preparative gel electrophoresis. J Chromatogr A 2007;1167:35–41.
[23] Chan WCW, Chithrani BD, Ghazani AA. Determining the size and shape dependence of gold nanoparticle uptake into mammalian cells. Nano Lett 2006;6:662–8.
[24] Lee D, Varnavski O, Ramakrishna G, Kim J, Goodson T. Critical size for the observation of quantum confinement in optically excited gold clusters. J Am Chem Soc 2010;132:16–7.
[25] de la Fuente JM, Berry CC. Tat peptide as an efficient molecule to translocate gold nanoparticles into the cell nucleus. Bioconjug Chem 2005;16:1176–80.
[26] de la Fuente JM, Berry CC, Riehle MO, Curtis ASG. Nanoparticle targeting at cells. Langmuir 2006;22:3286–93.
[27] Mosmann T. Rapid colorimetric assay for cellular growth and survival application to proliferation and cytotoxicity assays. J Immunol Methods 1983;65: 55–63.
[28] Lu WY, Liu M, Li C, Pazgier M, Li CQ, Mao YB, et al. D-peptide inhibitors of the p53-MDM2 interaction for targeted molecular therapy of malignant neoplasms. P Natl Acad Sci USA 2010;107:14321–6.
[29] Parak WJ, Sperling RA, Rivera gil P, Zhang F, Zanella M. Biological applications of gold nanoparticles. Chem Soc Rev 2008;37:1896–908.
[30] Xia YN, Cobley CM, Chen JY, Cho EC, Wang LV. Gold nanostructures: a class of multifunctional materials for biomedical applications. Chem Soc Rev 2011;40: 44–56.
[31] Boisselier E, Astruc D. Gold nanoparticles in nanomedicine: preparations, imaging, diagnostics, therapies and toxicity. Chem Soc Rev 2009;38:1759–82.
[32] Nadeau J, Zhang XA, Chibli H, Mielke R. Ultrasmall gold-doxorubicin conjugates rapidly kill apoptosis resistant cancer cells. Bioconjug Chem 2011;22: 235–43.
[33] Arosio D, Manzoni L, Araldi EMV, Scolastico C. Cyclic RGD functionalized gold nanoparticles for tumor targeting. Bioconjug Chem 2011;22:664–72.
[34] Kanaras AG, Bartczak D. Preparation of peptide functionalized gold nanoparticles using one pot EDC/Sulfo-NHS coupling. Langmuir 2011;27: 10119–23.